Supplementary Information

This Appendix contains the following supplementary information:

1. **Supplementary Materials and Methods**

2. **Supplementary Figures**

   Fig. S1. Screening and ranking strategy for DLBCL-subtype specificity.

   Fig S2. Dasatinib suppresses GCB-DLBCL cells in vivo.

   Fig. S3. Dasatinib suppresses Ibrutinib-resistant ABC-DLBCL in vivo.

   Fig. S4. PTEN inhibition induces Dasatinib resistance.

   Fig. S5. Constitutive PI3K activity induces Dasatinib resistance.

   Fig. S6. Dasatinib suppresses DLBCL-PDX derived cultures.

   Fig. S7. mTOR inhibitors are effective in all PTEN-negative Dasatinib-resistant cell lines.

3. **Supplementary Tables**

   Table S1. List of compounds ranked by DLBCL specificity.

4. **Supplementary Information References**.

Supplementary Materials and Materials

Drug screens. Nine cell lines (3 ABC: LY10, LY3 and HBL1; 3 GCB: SUDHL4, LY1 and BJAB; 3 MCL: JEKO-1, MINO and HBL2) were screened in 384-well format for 72 hours response to drug exposure. Cells were seeded at 1,000 cells/well and compounds applied after 24hrs. Viability was determined by Cell Titer-Glo assay (Promega). Two drug sets were screened: the Blau set and the Spectrum MicroDiscovery set. The Blau set consisted of 160 approved and investigational oncology drugs and included 45 FDA-approved drugs, while ~80% of the remaining compounds have been tested in early phase clinical trials. Drugs in this set were tested at 8 concentrations each in a 1:3 serial dilution ranging from 10 μM to 3.3nM in duplicate. The Spectrum MicroDiscovery set consisted of 2,000 drugs including 50% FDA approved principles. This set was first screened at 4 concentrations (10, 1, 0.1 and 0.01) and yielded 142 compounds with any activity on at least one cell line; these compounds were further validated at 8 concentrations each in duplicate as described for the Blau set.

Drug Specificity assessment. To assess subtype specificity, viability data were processed according to the following pipeline. First, viability duplicates at each concentration were averaged; data were then normalized to the lowest ineffective concentration. For each assay, a Sensitivity Area was calculated by adding the normalized viability parameter at each concentration and subtracting from the number of dose response points. Specificity scores for each compound were calculated by averaging Sensitivity Areas for all three cell lines for each of the other three groups (ABC-DLBCL, GCB-DLBCL and MCL) and then subtracting the scores for the remaining two groups. The DLBCL-specific scores were calculated by subtracting the MCL score from the ABC and GCB average.

Identification of predictors of resistance. A list of 2,109 mutational events including nonsynonymous mutations and copy number alterations was compiled for the whole cell panel from several sources(*1-6*). For each gene targeted at least twice, the difference between sensitivity averages of the resistant and sensitive lines was calculated and tested by Student t-test.

Dose response assay. For *in vitro* studies, 5,000 cells/well were plated in 96-well plates and treated with the indicated concentrations of Dasatinib, Ibrutinib, INK-128 or OSI-027 (Selleck) ranging from 10 mM to 1.5 nM. After 72 hours, viability was assessed by Cell Titer-Glo assay (Promega). Response at each dosage point is the average of four replicates. Curves were fitted with 5-point logistic (GraphPad). Error bars represent standard deviations. Dasatinib and Ibrutinib sensitivity thresholds were estimated on the basis of IC50 corresponding to maximum plasmatic concentrations for each compound (*7, 8*).

Combinatorial Studies. For combinatorial studies, cells were seeded in two 384-well plates at 1,000 cell/well by means of a Matrix WellMate microplate dispenser (Thermo Fisher Scientific). After 24 hours, drugs were pinned in a 10x10 matrix in 4 replicates each with a HP D300 digital dispenser (HP). Wells were normalized to the highest DMSO volume. Response was assessed after 72 hours by TiterGlo readings. To identify concentration ranges at which synergy occurred Highest Single Agent (HSA) models were generated with Combenefit (*9*) and five-point logistic curves were fitted for the two compounds alone and in combination with the concentrations at which synergy was detected according to the model. EC50 were then derived for all relevant conditions and combinatorial indexes were calculated according to the method of Chou and Talay(*10*).

Cell lines. LY4 and LY10 were grown in IMDM supplemented with 55 µM Beta-Mercaptoethanol, 20% Human Plasma (New York Blood Bank) and 1% Penicillin/Streptomycin. All other cell lines used in this study were grown in IMDM supplemented with 10% Fetal Bovine

Serum and 1% Penicillin/Streptomycin. 293T cells were grown in DMEM media supplemented with 10% Fetal Bovine Serum and 1% Penicillin/Streptomycin. The cell line FARAGE shares similarities with PMBL and it is therefore indicated as DLBCL/PMBL (*11*).

Lentivirus production. All vectors described in this study were cloned with standard molecular biology techniques. cDNA were constitutively expressed from UBC promoters (*12*) and linked to fluorescent proteins by means of P2A peptides (*13*). All lentiviruses were produced in 293T cells by calcium phosphate co-transfection of lentiviral vectors with packaging vector PSPAX2 (a gift from Didier Trono; Addgene plasmid # 12260) and pMD2.G (Addgene #12259). Viral supernatants were collected at 40hrs, filtered with a 0.45 µM filter and supplemented with polybrene (8 µg/ml, Sigma). 250,000 target cells were spinoculated for 60 minutes at 1,900 rpm. Virus collection and infection were repeated after 12 hours. After 24 hours, cells were washed in growing media, grown for additional 24 hours and sorted according to the tagged fluorescence by using a FACS Aria sorter (BD Biosciences).

Western Blot assays. Five million cells per sample were washed in cold PBS and lysed in 1% Triton lysis Buffer (150 mM NaCl, 1mM EDTA, 1mM EGTA, 20 mM Tris pH 6.8 supplemented with Protease Inhibitor Cocktail (Sigma), 1 mM NaF, 1 mM beta-glycerophosphate, 1 mM PMSF, 1 mM Sodium Orthovanandate). Protein lysates were subjected to SDS-PAGE and transferred to nitrocellulose membranes (Amersham). The following primary antibodies were used: phospho-473 AKT (CST #9271), pan-AKT (CST #4691), phospho-223 BTK (Abcam #ab68217), HA (Roche #11867423001). For IP experiments, 10 million cells were washed in cold PBS and lysed in IP buffer (25 mM Tris-HCl pH 7.5, 100 mM NaCl, 1 mM EDTA, 1% Triton, 0.05% NP40 supplemented with inhibitors as described above). 500 µg of proteins were subject to IP O/N with Red-View Sepharose HA beads (Sigma) according to the manufacturer instructions. Beads were

washed three time with ice cold buffer, resuspended in Laemmli buffer and subject to SDS-PAGE and Western Blot. Blots were visualized using ECL (Pierce #32106) followed by film exposure. Image densitometry was performed with Fiji (*14*).

Animal Studies. All animal experiments were approved by the Institutional Animal Care and Use Committee. DLBCL lines were lentivirally transduced to express a Luciferase-Tomato fusion protein (Addgene #32904). $1*10^7$ cells were diluted in PBS, mixed 1:1 with Matrigel (Corning #356230) and injected s.c. in NOD/SCID mice (Jackson Laboratory). Recipient mice were monitored by Luciferase imaging and palpation. For imaging, mice were injected with XenoLight D-Luciferin (15 mg/ml in PBS, Perkin Elmer) at 150mg/kg, anesthetized with 2.5% isoflurane and imaged with an IVIS Spectrum Optical Imaging System. Mice carrying tumors that were palpable (>2 mm) and with radiance greater than $1*10^7$ luc photons were randomly assigned to vehicle or treatment(s) cohorts. Drugs for *in vivo* use were purchased from LC Laboratories. Dasatinib was resuspended in 80 mM Citric Acid pH 3.1 (*15*) and administered at 10 mg/kg twice daily. Ibrutinib was dissolved in 20% beta-cyclodextrin (Sigma) and diluted in saline solution for dosing at 12.5 mg/kg daily. For INK128, stock solutions were prepared first by dissolving the drug in NMP (1-Methyl 2-pyrrolidinone, Sigma) at 20 mg/ml; for dosing, stock solutions were dissolved in 15% PVP (Polyvinylpyrrolidone, Sigma) to 0.2 mg/ml and administered at 0.75 mg/kg with alternate schedule. All drugs were administered by oral gavage. For defining progression-free survival, a tumor diameter of 20 mm was used as survival endpoint according to the approved protocol.

Statistical Analysis. Dose response curves were fitted using five-point logistics (Graph Pad). For each concentration point 4 replicates were averaged to generate the response function. Response point greater than 20% of the control were set to 1.2 (control=1). Error bars for individual response point represent standard deviation. P-values refers to unpaired t-test

(*p<0.05;**p<0.01;***p<0.001) of normalized viability at the indicated concentrations. Significance of survival difference was assessed by log-rank test.

Supplementary Figures

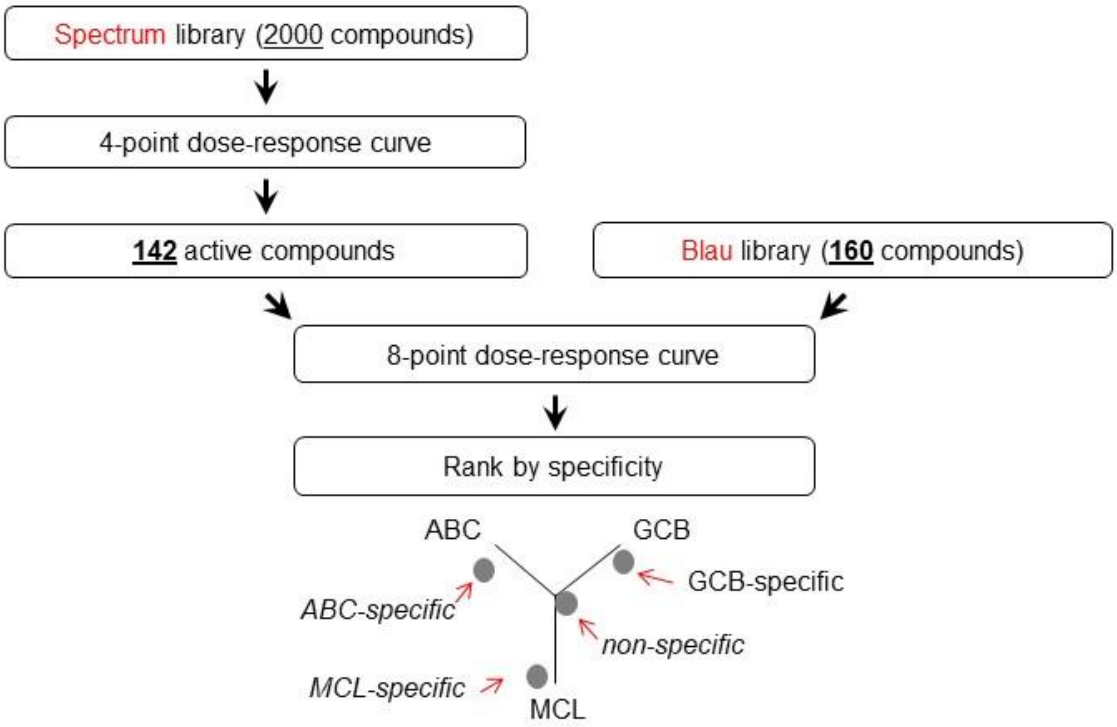

Fig. S1. *Screening and ranking strategy for DLBCL-subtype specificity*. Outline of the screening and prioritization pipeline. Spectrum library compounds were screened with a five-point dose response. Compounds showing any kind of activity in any cell line were re-tested in 8-point dose response. The Blau library compounds were screened directly in the 8-point dose response. The resulting 302 compounds were then ranked by subtype specificity and plotted accordingly (see Fig. 1 and table S1).

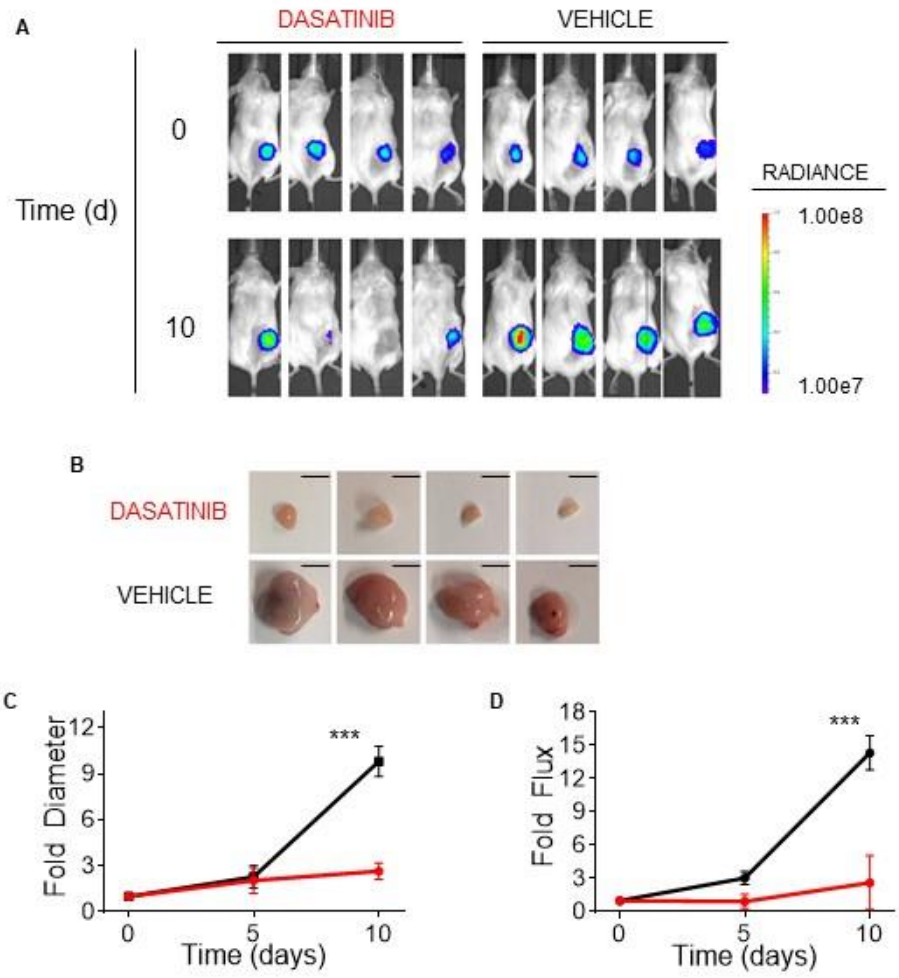

Fig. S2. *Dasatinib suppresses GCB-DLBCL cells in vivo*. (A) Luciferase imaging at day 0 and 10 of NOD/SCID mice subcutaneously transplanted with WSU-NHL cells carrying a Luciferase Tomato expressing vector and treated with Dasatinib (10 mg/kg twice daily) or vehicle only. (B) Resections of subcutaneous tumors from Dasatinib-treated, or vehicle only animals at day 10. Bar, 10 mm. Fold change of diameter (C) flux and flux (D) over time relative to time 0 for Dasatinib-treated (red) or vehicle only (black) WSU-NHL xenotransplants. Error bars represent standard deviations (***$p<0.001$, T-test; n=4 mice per group).

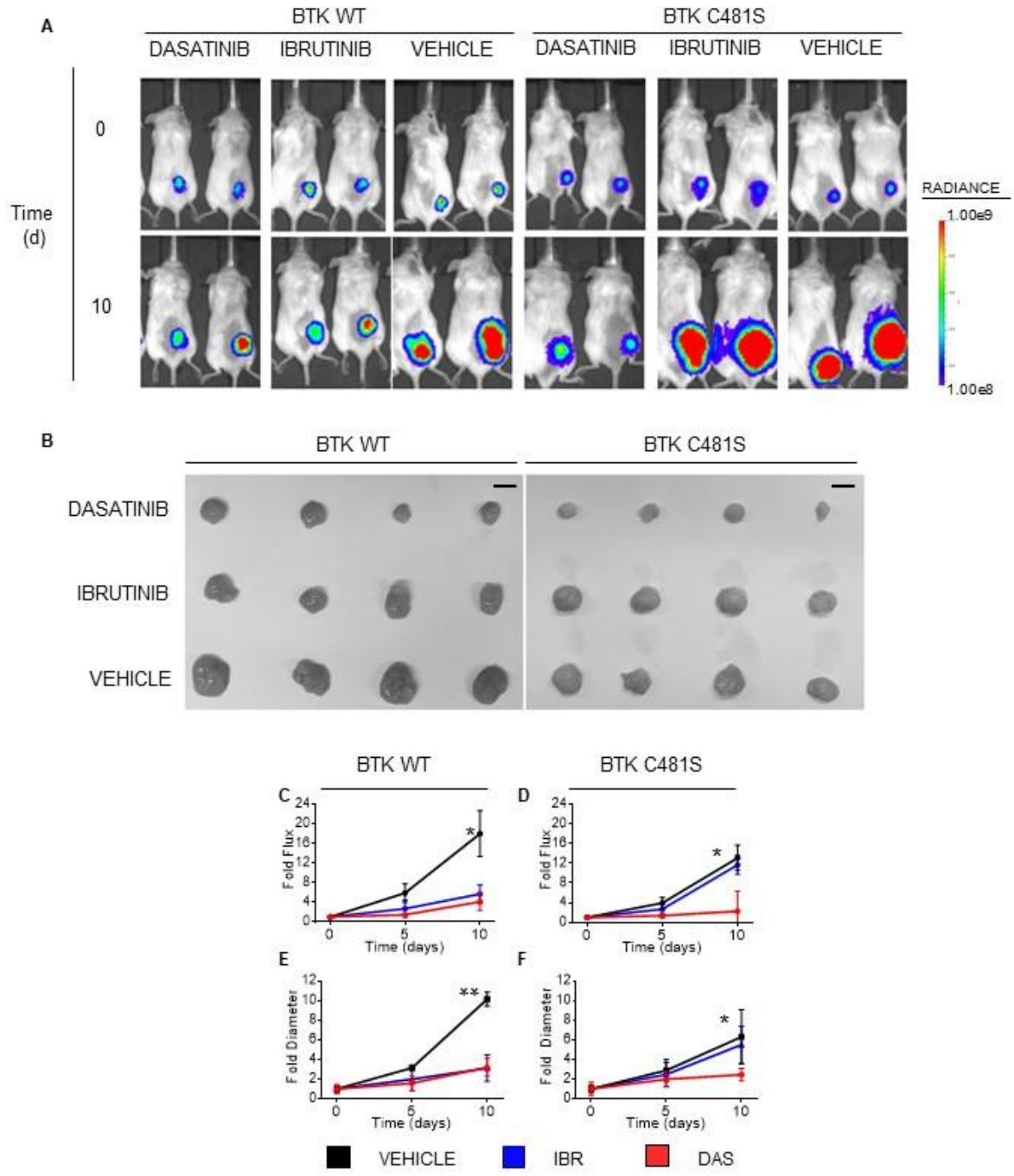

Fig. S3. *Dasatinib suppresses Ibrutinib resistant ABC-DLBCL cells in vivo*. (A) Luciferase imaging of NOD/SCID mice subcutaneously transplanted with HBL1 cells carrying a Luciferase Tomato expressing vector (HBL1 LTS) and a vector encoding BTK WT or BTK C481S, and treated with Dasatinib (10 mg/kg twice daily), Ibrutinib (12 mg/kg/d) or vehicle only. (B)

Resections of subcutaneous tumors in Dasatinib-treated, Ibrutinib-treated, or vehicle only at day 10. Bar, 10 mm. Fold change of (C-D) flux and diameter (E-F) over time relative to time 0 for Dasatinib-treated (red), Ibrutinib-treated (blue) or vehicle only (black) HBL1-LTS BTK WT or BTK C481S xenotransplants. Error bars represent standard deviations (*$p<0.05$;**$p<0.01$, T-test; n=4 mice per group).

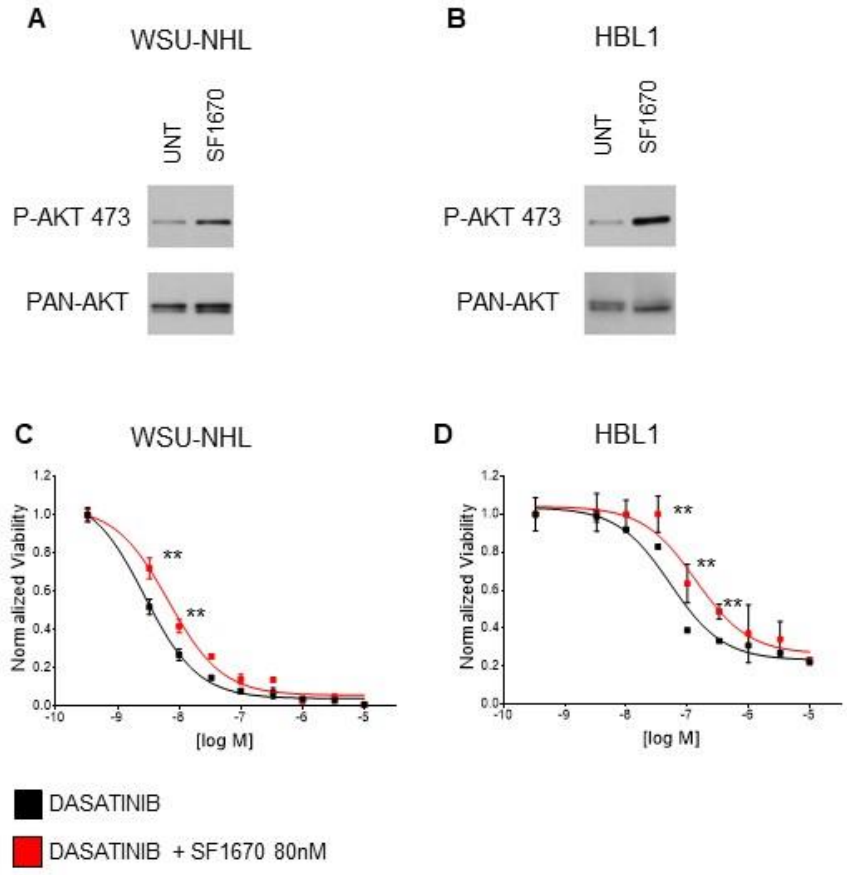

Fig. S4. *PTEN inhibition induces Dasatinib resistance*. (A-B**)**. Western Blot analysis for AKT S473 phosphorylation in WSU-NHL (A) and HBL1 (B) in cell left untreated or treated with the 2 µM PTEN inhibitor SF1670 for one hour. Dose response assay to Dasatinib alone (black) and Dasatinib in the presence of 80 nM SF1670 (red) in WSU-NHL (C) and HBL1 (D) cells. Error bars represent standard deviations (n=4 replicates/dosage point; **p<0.01; Student t-test).

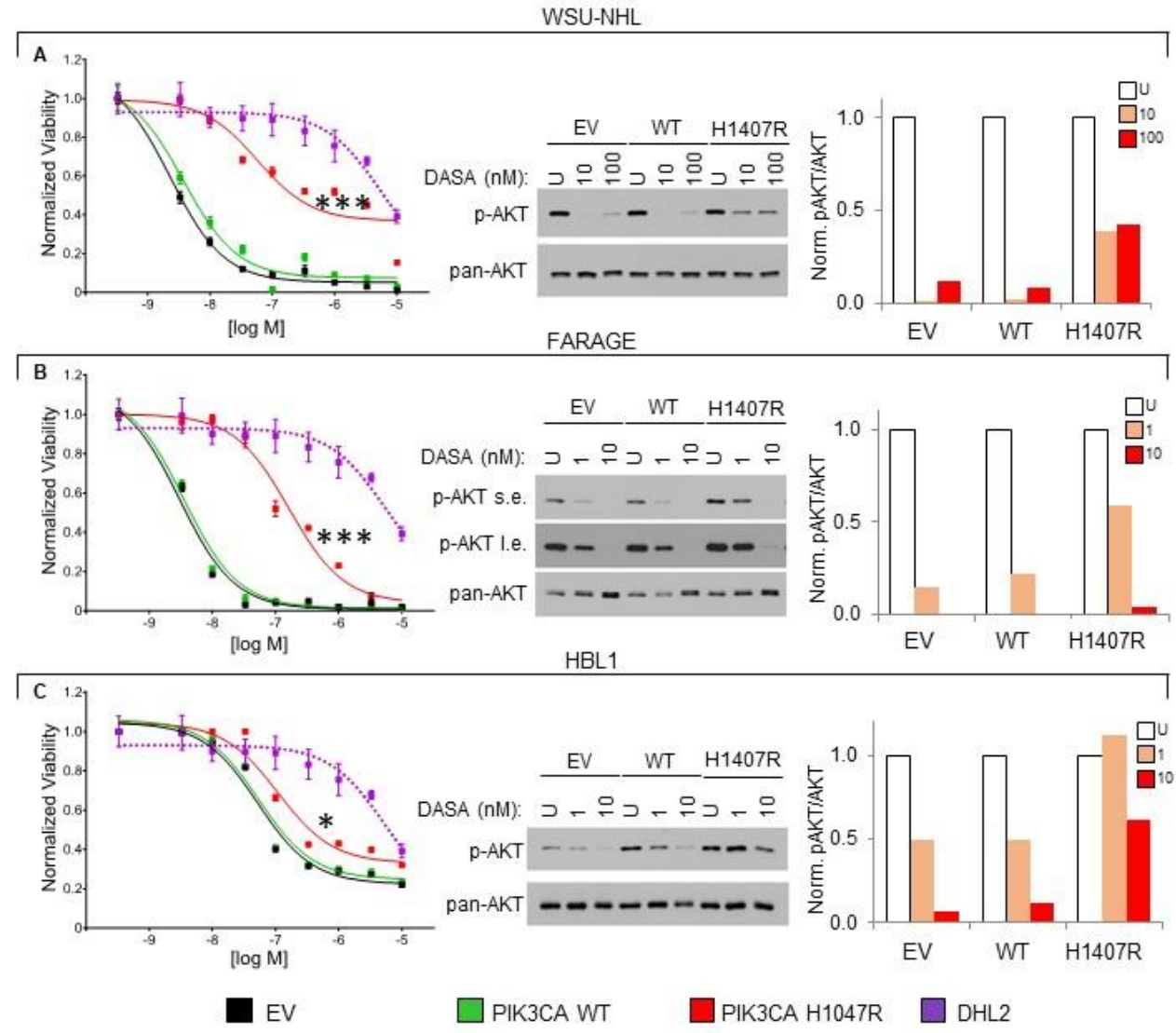
WSU-NHL
A
Normalized Viability
[log M]
***
EV
WT
H1407R
DASA (nM):
U
10
100
p-AKT
pan-AKT
Norm. pAKT/AKT
FARAGE
B
1
HBL1
C
*
EV
PIK3CA WT
PIK3CA H1047R
DHL2

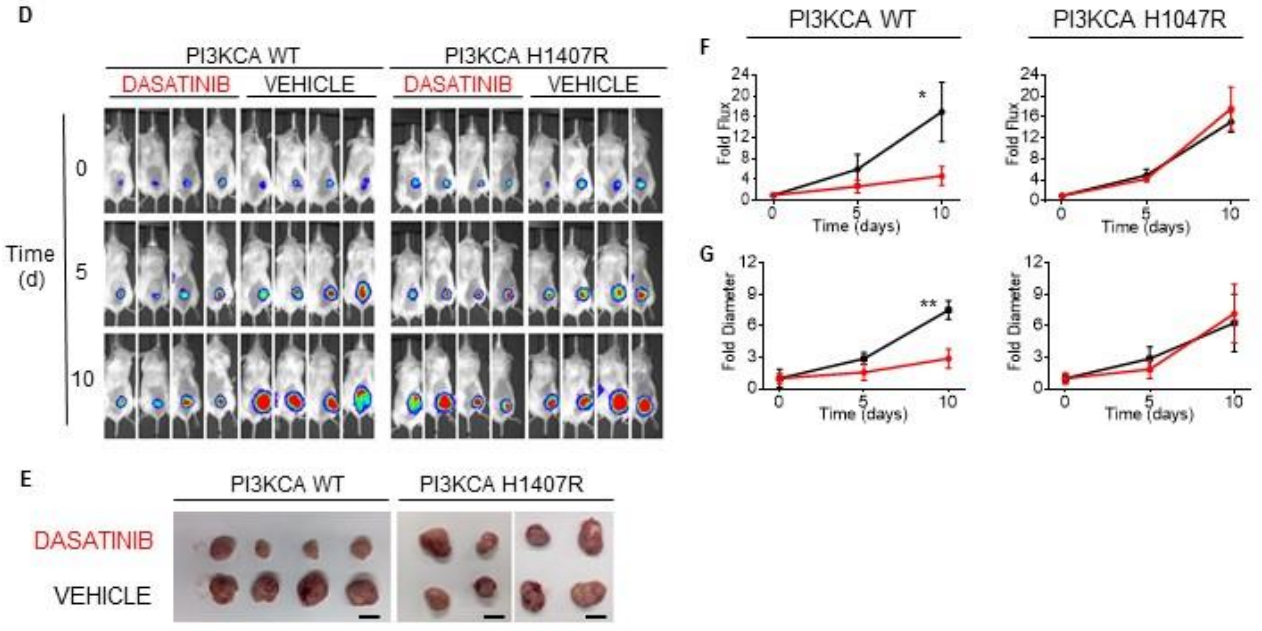
D
PI3KCA WT
PI3KCA H1407R
DASATINIB
VEHICLE
Time (d)
0
5
10
E
DASATINIB
VEHICLE
F
Fold Flux
Time (days)
G
Fold Diameter
**

Fig. S5. *Constitutive PI3K activity induces Dasatinib resistance.* WSU-NHL (A), FARAGE (DLBCL/PMBL, B) and HBL1 (C) cells were transduced with an empty vector (EV, black), or vectors expressing PI3KCA wild-type (WT, green) or a PI3KCA constitutively active mutant (H1047R, red) and tested for Dasatinib sensitivity (*left panels*). The DHL2 cell line (dashed violet line) is used as reference for Dasatinib resistance. Statistics indicate t-test for PI3KCA 1047R compared to PI3KCA WT; *p<0.05; ***p<0.001. *Middle panels*; AKT S473 phosphorylation was analyzed by immunoblotting in EV, WT and H1047R cells treated at two Dasatinib concentrations (10 and 100 nM for WSU-NHL; 1 and 10 nM for FARAGE and HBL1) or left untreated (U). Pan-AKT was used for normalization. Quantification of AKT activation (phospho-AKT S473/pan-AKT) normalized to untreated cells in response to the indicated Dasatinib treatments is shown in the right panels. (D) Luciferase imaging at day 0, 5 and 10 of mice transplanted s.c. with luciferized HBL1 cells modified to express PI3KCA wild-type (WT) or the constitutively active H1047R mutant, and treated with Dasatinib (10mg/kg twice daily) or vehicle only. (E) Lymphoma resections from the treatment conditions shown above. Bar, 10mm. (F) Flux and (G) tumor diameter fold changes relative to time 0 in mice treated with Dasatinib (red) or vehicle (black) carrying lymphomas expressing PIK3CA WT (left) or H1047R (right) (**p<0.05; n=4/group).

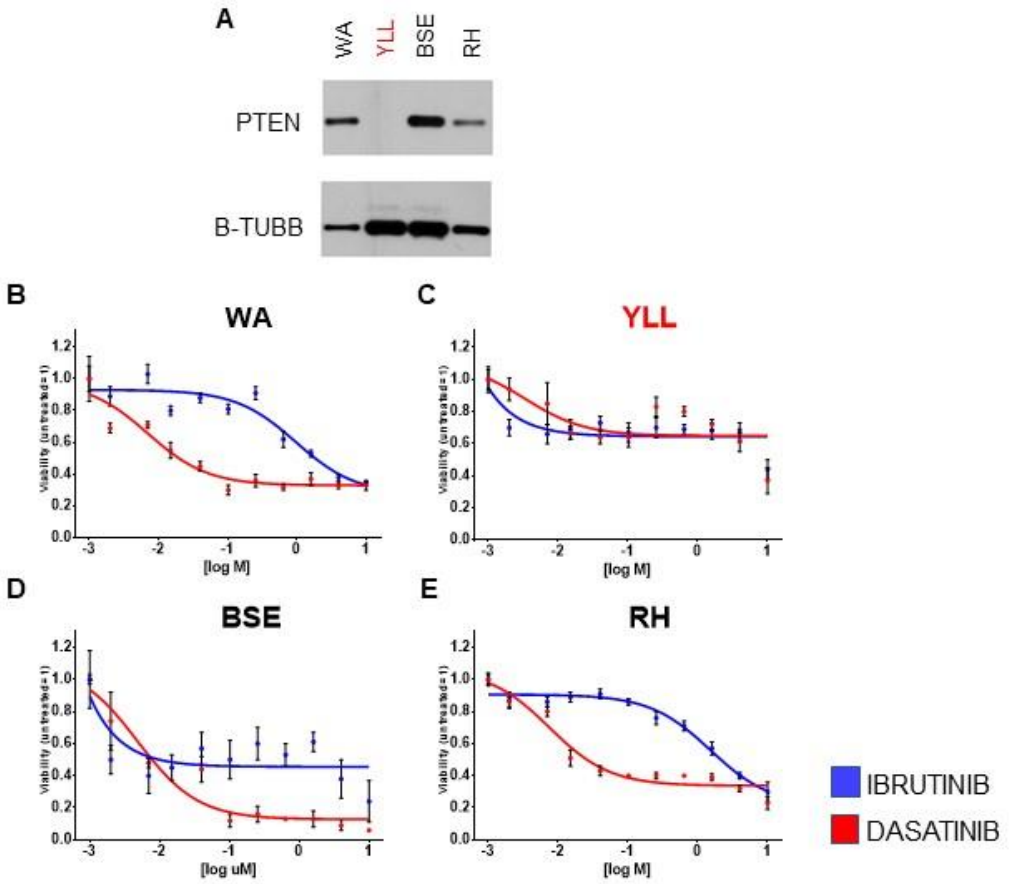

Fig. S6. *Dasatinib suppresses DLBCL PDX-derived cultures*. (A) Western Blot analysis for PTEN expression in 4 PDX cultures. (PTEN negative, red). (B-E) Ibrutinib (blue) and Dasatinib (red) dose response assays for the 4 ex-vivo PDX models. Error bars represent standard deviations (n=4 replicates/dosage point). RH derives from a Richter Syndrome (RS) patient initially treated with Ibrutinib.

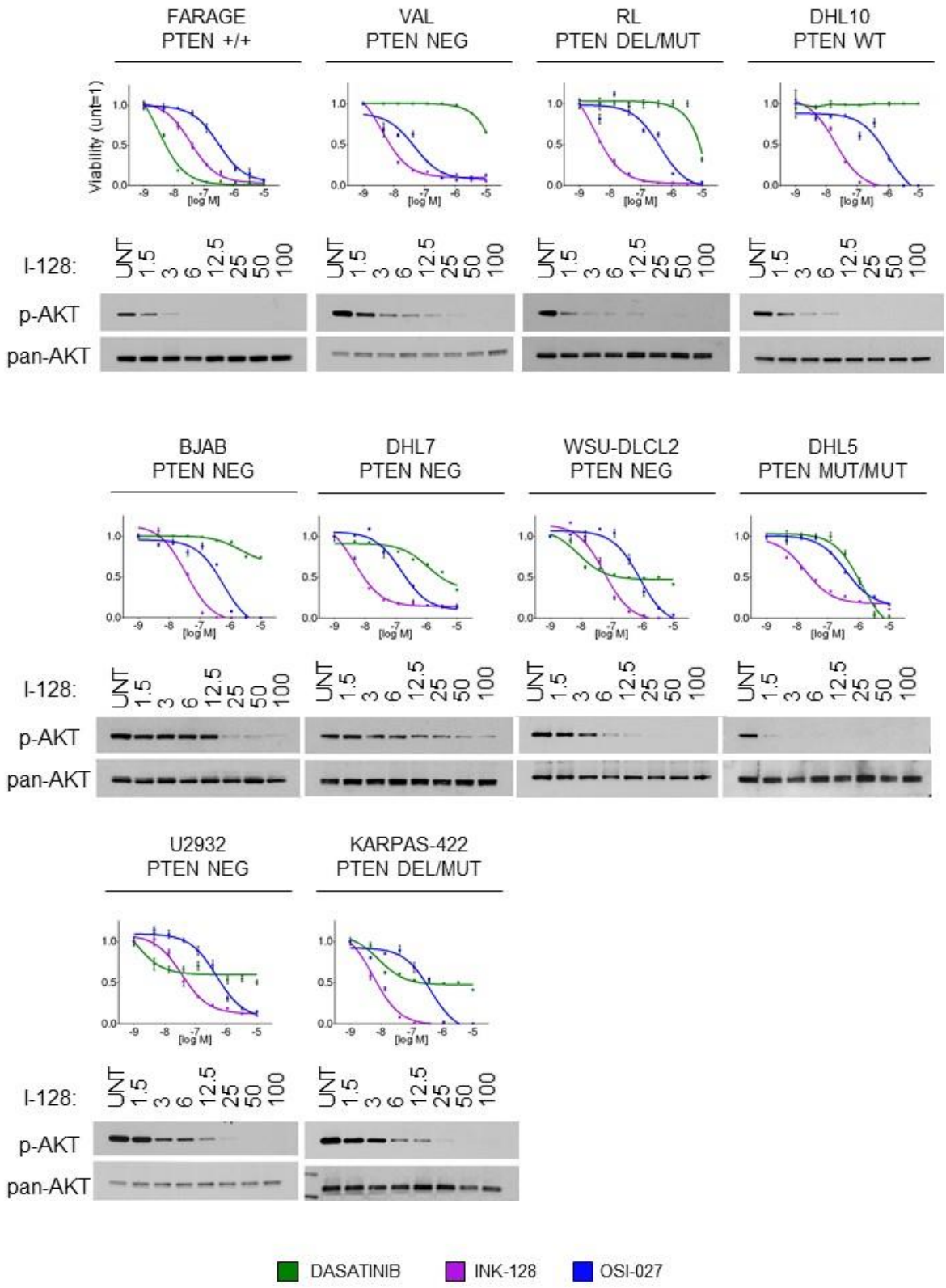

Fig. S7. *mTORC inhibitors are effective in all PTEN-negative Dasatinib-resistant cell lines*. Dose

response curves for Dasatinib-resistant, AKT-positive cell lines (n=9) treated with Dasatinib (green), OSI-027 (blue) or INK-128 (violet). PTEN status is indicated for each cell line. The Dasatinib-sensitive line Farage (DLBCL/PMBL) is shown as Dasatinib-sensitive positive control. Below, AKT S473 phosphorylation upon treatment with the indicated INK-128 concentrations (nM) or left untreated (U). Bars for dose response points represent standard deviations (n=4 replicates/point).

Table S1. List of compounds ranked by DLBCL specificity.

Compound	SCORES				
	DLBCL	**ABC**	**GCB**	**MCL**	**ABC (vs GCB)**
Dasatinib	383	273	109	-383	109
Fluorometholone	258	155	102	-258	35
Flurandrenolide	241	187	54	-241	88
Dexamethasone Sodium Phosphate	238	95	142	-238	-31
Rapamycin	232	120	112	-232	4
Fludarabine	229	128	100	-229	18
Temsirolimus	221	120	100	-221	13
Betamethasone	221	160	60	-221	67
Everolimus	217	129	88	-217	27
Panobinostat	211	91	120	-211	-19
Flunisolide	199	118	81	-199	24
Bleomycin	193	176	16	-193	106
Gdc-0941	187	107	80	-187	18
2,3-Dihydroxy-4-Methoxy-4'-Ethoxybenzophenone	180	78	102	-180	-16
Osi-027	179	-57	237	-179	-196
Tg-101348	179	97	82	-179	9
Etoposide	179	113	65	-179	32
Dexamethasone Acetate	177	92	85	-177	4
Fluocinolone Acetonide	175	83	92	-175	-6
Sirolimus	167	92	75	-167	11
Pp-242	163	108	55	-163	35
Methotrexate	158	83	74	-158	5
Clobetasol Propionate	156	181	-25	-156	137
Sulindac	149	23	125	-149	-68
Pi-103	147	47	100	-147	-35
Osi-906	144	98	46	-144	34
Pik-90	143	174	-31	-143	137
Epirubicin Hydrochloride	138	33	105	-138	-48
Bgt-226	129	20	108	-129	-59
Tipifarnib	126	-49	175	-126	-150
Azd-8055	122	28	93	-122	-43

Pki-587	121	19	102	-121	-55
Ap24534	112	-30	142	-112	-115
Thioguanine	111	121	-10	-111	88
Nvp-Lde-225	110	-27	138	-110	-110
Teniposide	109	6	103	-109	-64
Pf-04691502	108	71	37	-108	22
Mercaptopurine	104	66	37	-104	19
Ski-606	94	85	9	-94	50
Brompheniramine Maleate	93	58	34	-93	16
Bez-235	91	-33	124	-91	-105
Salinomycin, Sodium	90	-116	207	-90	-215
Clofarabine	90	-45	135	-90	-120
Hydralazine Hydrochloride	90	21	69	-90	-32
Cal-101	86	40	45	-86	-3
As101	81	-67	148	-81	-143
Sns-032	80	70	10	-80	39
Azathioprine	74	34	40	-74	-3
3,7-Dimethoxyflavone	72	-61	134	-72	-130
Mln8237	72	127	-55	-72	122
Labetalol Hydrochloride	67	67	0	-67	44
Vorinostat	67	121	-53	-67	116
Temozolomide	67	124	-57	-67	121
Clotrimazole	65	24	40	-65	-11
Azd0530	65	29	35	-65	-3
Lenalidomide	65	96	-31	-65	85
Tgx-221	64	40	24	-64	10
Tamoxifen	64	49	15	-64	22
Mk2206	62	-45	107	-62	-101
Pemetrexed	62	64	-2	-62	44
Cyclosporine	61	-2	63	-61	-43
Vandetanib	61	12	49	-61	-24
Zstk-474	60	-68	129	-60	-131
3,4'-Dimethoxyflavone	59	-74	134	-59	-139
Gramicidin	58	-86	144	-58	-153
Arsenic Trioxide	58	101	-42	-58	96
Rdea-119	57	76	-18	-57	63
Lomustine, Ccnu	57	96	-38	-57	90
Monensin Sodium (Monensin A Is Shown)	55	-130	185	-55	-210
Cisplatin	54	66	-11	-54	52
Otava 7015980251	53	23	30	-53	-4

Pik-75	52	51	0	-52	34
Carboplatin	52	87	-35	-52	81
Chloroacetoxyquinoline	51	-71	122	-51	-129
Azd7762	51	20	30	-51	-6
Mitoxantrone	51	23	28	-51	-3
Melphalan	51	151	-99	-51	167
Estrone Benzoate	50	-58	108	-50	-111
Daunorubicin Hcl	50	42	7	-50	23
Hydroxyurea	50	51	0	-50	34
Sorafenib	50	65	-15	-50	54
Flavopiridol	48	-1	49	-48	-33
Busulfan	48	39	9	-48	19
Fti-276	48	53	-4	-48	38
Acarbose	47	-27	75	-47	-68
4'-Methoxychalcone	46	-93	140	-46	-156
Piplartine	46	2	44	-46	-28
Homidium Bromide	46	25	21	-46	2
Pazopanib	46	107	-61	-46	112
Salicin	45	-44	89	-45	-89
Gant58	45	37	8	-45	19
Plx-4032	44	32	12	-44	13
Thalidomide	43	48	-5	-43	35
Acrichine	42	82	-39	-42	81
Idazoxan Hydrochloride	41	-51	92	-41	-95
R-Roscovitine	41	32	8	-41	15
Mg132	41	66	-24	-41	60
Tyrothricin	39	-69	109	-39	-119
Patulin	38	15	22	-38	-4
Belinostat	38	65	-26	-38	61
Garlicin	37	-17	55	-37	-49
Piscidic Acid	37	-3	40	-37	-29
Sb 218078	37	55	-17	-37	48
2,3-Dichloro-5,8-Dihydroxynapthoquinone	36	58	-21	-36	53
Ac-220	35	23	11	-35	7
Canthaxanthin (Euglenanone)	34	-55	90	-34	-97
Tpca-1	34	126	-91	-34	145
3Beta-Hydroxy-23,24-Bisnorchol-5-Enic Acid	33	-30	63	-33	-62
3,4',5,6,7-Pentamethoxyflavone	33	-14	48	-33	-42
Gefitinib	33	47	-13	-33	40
Lapatinib	32	14	17	-32	-1

Gf109203X	32	65	-32	-32	65
Tenoxicam	31	-66	98	-31	-109
Amiodarone Hydrochloride	31	-65	96	-31	-108
Osajin	31	-1	33	-31	-23
Arq-197	31	13	17	-31	-2
Itraconazole	30	-93	123	-30	-144
Helenine	30	-39	69	-30	-72
Norgestimate	29	-61	90	-29	-101
Pravastatin	29	48	-18	-29	44
Sgi-1776	28	33	-5	-28	25
Vatalanib	28	54	-26	-28	54
Isaxonine	27	-38	65	-27	-69
Bkm-120	27	55	-28	-27	56
Parthenolide	26	-5	32	-26	-24
Azacitidine	26	28	-2	-26	20
Pentostatin	26	44	-17	-26	41
Pararosaniline Pamoate	25	-61	86	-25	-98
Acadesine	25	-6	32	-25	-26
Sunitinib	25	31	-6	-25	25
Plx-4720	25	34	-9	-25	29
Valproic Acid	25	50	-24	-25	50
Albendazole	24	-57	82	-24	-93
Deguelin(-)	24	-25	49	-24	-49
Beta-Peltatin	24	1	22	-24	-14
Tki258	23	17	6	-23	7
Xl-147	22	43	-21	-22	42
Disulfiram	21	-38	60	-21	-65
C3742	21	36	-14	-21	33
Pha-793887	20	52	-31	-20	56
Fumarprotocetraric Acid	19	-87	106	-19	-129
Pf-04217903	19	31	-11	-19	28
5-Iodotubercidin	19	68	-48	-19	78
Nilotinib	18	37	-19	-18	37
As-605240	18	46	-27	-18	49
7-Desacetoxy-6,7-Dehydrogedunin	17	-26	44	-17	-47
Dbz	16	42	-26	-16	45
Sb-431542	16	45	-29	-16	50
Tamibarotene	15	25	-10	-15	24
Tandutinib	15	40	-24	-15	43
Gdc-0449	15	42	-27	-15	46

Benzyl Isothiocyanate	14	-61	75	-14	-91
2-Methyl-5,7,8-Trimethoxyisoflavone	14	-29	43	-14	-48
Thiram	14	-1	16	-14	-11
Bay 11-7082	14	25	-11	-14	24
Chlorhexidine	14	31	-17	-14	32
Medroxyprogesterone Acetate	12	-47	60	-12	-72
Clomipramine Hydrochloride	12	3	8	-12	-2
Harmine	12	16	-3	-12	13
4-Methyldaphnetin	12	18	-5	-12	15
Tanespimycin	12	21	-9	-12	21
4'-Demethylepipodophyllotoxin	12	23	-11	-12	23
Azd-6244	12	68	-56	-12	83
Alexidine Hydrochloride	11	-37	48	-11	-57
Bibw 2992	11	19	-8	-11	18
Bay 11-7085	11	24	-12	-11	24
Etodolac	11	47	-36	-11	55
Isorotenone	10	-25	36	-10	-40
Bortezomib	10	30	-19	-10	33
Olaparib	9	-101	110	-9	-141
Pindolol	9	-8	17	-9	-17
Incb-018424	9	28	-19	-9	31
U 73122	9	30	-20	-9	34
Totarol Acetate	8	-32	41	-8	-49
Irigenin	8	42	-34	-8	51
Abt-888	8	43	-34	-8	52
Mexiletine Hydrochloride	7	-68	75	-7	-96
Gambogic Acid	7	-46	53	-7	-66
Ic-87114	7	22	-14	-7	24
Emd-1214063	7	39	-31	-7	47
As-703026	7	49	-42	-7	61
Pkc412	5	64	-58	-5	81
Mubritinib	4	-54	58	-4	-75
2,6-Dimethoxyquinone	3	-37	41	-3	-52
Picropodophyllin	3	-25	28	-3	-36
Vinblastine Sulfate	3	-1	5	-3	-4
At-7519	3	0	3	-3	-2
2',4'-Dihydroxy-4-Methoxychalcone	2	-44	46	-2	-60
Enzastaurin	2	40	-38	-2	53
2',4-Dihydroxychalcone	0	-78	78	0	-104
Deoxygedunin	0	22	-22	0	30

Gsk-1120212	0	63	-64	0	84
Azd8330	0	81	-81	0	108
Tozasertib	0	102	-103	0	137
Plumbagin	-1	-79	77	1	-104
Bendroflumethiazide	-1	1	-3	1	3
Phps1	-1	29	-31	1	40
Ym-155	-2	-3	0	2	-2
Aminacrine	-3	-62	59	3	-81
Diallyl Trisulfide	-3	4	-7	3	8
Vincristine Sulfate	-4	-4	0	4	-3
Deoxysappanone B 7,4'-Dimethyl Ether	-5	-71	66	5	-91
3-Bromo-4-Methyl-3,4-Hexamethylene-3,4-Dihydrodiazete-1.2-Dioxide	-5	-51	45	5	-64
Bsi-201	-5	28	-33	5	41
Thiabendazole	-6	-45	38	6	-56
3,4-Dimethoxydalbergione	-6	-40	34	6	-49
Podofilox	-6	-34	28	6	-42
2',4'-Dihydroxychalcone	-6	-32	25	6	-38
Deoxysappanone B 7,3'-Dimethyl Ether Acetate	-7	-88	81	7	-113
Dihydrotanshinone I	-7	14	-21	7	24
Crizotinib	-7	30	-38	7	46
Erlotinib Hcl	-8	-6	-2	8	-2
Convallatoxin	-8	8	-16	8	16
Digoxigenin	-8	20	-28	8	32
Emetine	-9	1	-11	9	8
Amiloride Hydrochloride	-9	10	-19	9	20
Not Available	-10	22	-33	10	37
Mitoxantrone Hydrochloride	-10	31	-42	10	49
Bms-754807	-10	60	-70	10	87
Bi-2536	-11	-15	4	11	-12
Prazosin Hydrochloride	-14	-57	42	14	-66
Deferoxamine Mesylate	-14	-51	37	14	-59
Strophanthidinic Acid Lactone Acetate	-14	-14	0	14	-9
Bms-708163	-15	20	-36	15	37
Astemizole	-17	-42	25	17	-45
Otava 1112092	-17	4	-22	17	18
Irinotecan Hcl	-17	28	-46	17	50
Anisomycin	-18	-29	10	18	-26
Bml 277	-18	17	-35	18	35
Dalbergione	-19	-57	38	19	-64

Otava 7070707035	-19	-36	16	19	-35
Fucostanol	-19	-34	15	19	-33
Harmaline	-20	-25	5	20	-20
Isoetharine Mesylate	-20	19	-40	20	39
E7080	-20	25	-45	20	47
Otava 0107830108	-20	31	-51	20	55
3,4-Didesmethyl-5-Deshydroxy-3'-Ethoxyscleroin	-21	-57	36	21	-62
Anthothecol	-21	-54	33	21	-58
Cedrelone	-21	-14	-7	21	-4
Vinorelbine Tartrate	-21	16	-37	21	36
Nvp-Tae-684	-21	27	-48	21	50
2,5-Di-T-Butyl-4-Hydroxyanisole	-23	8	-32	23	27
Apomorphine Hydrochloride	-24	-14	-9	24	-3
Antiarol	-26	-45	19	26	-42
Oxibendazole	-26	-41	14	26	-37
Pristimerin	-27	-58	31	27	-59
Tosedostat	-27	-14	-12	27	-1
Podophyllin Acetate	-28	-61	33	28	-63
7,8-Dihydroxyflavone	-28	-27	0	28	-18
Amodiaquine Dihydrochloride	-28	4	-32	28	24
Bibf1120	-28	20	-48	28	46
Otava 7020402324	-28	24	-52	28	51
Baicalein	-30	-99	69	30	-112
Peruvoside	-31	-19	-12	31	-4
Acriflavinium Hydrochloride	-34	-54	19	34	-48
Digitoxin	-35	-59	23	35	-55
Digoxin	-35	-39	3	35	-28
Acetyl Isogambogic Acid	-36	-113	77	36	-127
Pd-0325901	-37	-14	-23	37	6
Phenethyl Caffeate (Cape)	-38	52	-90	38	95
Alrestatin	-40	-65	25	40	-60
Dihydrocelastryl Diacetate	-42	-71	28	42	-66
Avocatin A	-43	-63	19	43	-55
Fenretinide	-43	2	-45	43	31
Axitinib	-44	13	-57	44	47
Ms-275	-44	78	-123	44	134
Dihydrocelastrol	-46	-80	34	46	-76
Niclosamide	-46	-46	0	46	-30
Gitoxin	-46	10	-57	46	45
Gitoxigenin Diacetate	-47	-64	16	47	-54

10-Hydroxycamptothecin	-47	-56	9	47	-44
Mitomycin C	-49	83	-132	49	144
Azd2171	-50	-2	-47	50	30
Topotecan Hcl	-53	-30	-22	53	-5
Masitinib	-53	-14	-38	53	16
Camptothecin	-54	-158	103	54	-174
Monobenzone	-55	-49	-5	55	-29
Avocadyne Acetate	-58	-32	-25	58	-4
Bexarotene	-60	0	-59	60	39
Pd0332991	-65	3	-69	65	48
3-Methoxycatechol	-66	-70	3	66	-49
Cholecalciferol	-68	-117	48	68	-110
Tretinoin	-69	2	-71	69	49
Avocatin B	-75	-66	-8	75	-38
Staurosporine	-98	-77	-20	98	-37
Obatoclax	-105	-31	-73	105	27
Abt-263	-109	-59	-49	109	-6
Decitabine	-115	-119	3	115	-81
Abt-737	-117	-31	-86	117	36
Nvp-Auy-922	-126	-56	-69	126	8
Kinetin Riboside	-141	-57	-84	141	17
Ancitabine Hydrochloride	-191	-37	-153	191	77
Gemcitabine Hcl	-195	-135	-60	195	-49
Floxuridine	-215	33	-248	215	187
Cytarabine Hcl	-219	-67	-151	219	55
On 01910.Na	-253	-118	-135	253	11
Paclitaxel	-273	-121	-152	273	20
Cladribine	-330	-86	-243	330	104

SI Appendix References

1. J. Barretina, G. Caponigro, N. Stransky, K. Venkatesan, A. A. Margolin, S. Kim, C. J. Wilson, J. Lehar, G. V. Kryukov, D. Sonkin, A. Reddy, M. Liu, L. Murray, M. F. Berger, J. E. Monahan, P. Morais, J. Meltzer, A. Korejwa, J. Jane-Valbuena, F. A. Mapa, J. Thibault, E. Bric-Furlong, P. Raman, A. Shipway, I. H. Engels, J. Cheng, G. K. Yu, J. Yu, P. Aspesi, Jr., M. de Silva, K. Jagtap, M. D. Jones, L. Wang, C. Hatton, E. Palescandolo, S. Gupta, S. Mahan, C. Sougnez, R. C. Onofrio, T. Liefeld, L. MacConaill, W. Winckler, M. Reich, N. Li, J. P. Mesirov, S. B. Gabriel, G. Getz, K. Ardlie, V. Chan, V. E. Myer, B. L. Weber, J. Porter, M. Warmuth, P. Finan, J. L. Harris, M. Meyerson, T. R. Golub, M. P. Morrissey, W. R. Sellers, R. Schlegel, L. A. Garraway, The Cancer Cell Line Encyclopedia enables predictive modelling of anticancer drug sensitivity. *Nature* **483**, 603-607 (2012).

2. M. Compagno, W. K. Lim, A. Grunn, S. V. Nandula, M. Brahmachary, Q. Shen, F. Bertoni, M. Ponzoni, M. Scandurra, A. Califano, G. Bhagat, A. Chadburn, R. Dalla-Favera, L. Pasqualucci, Mutations of multiple genes cause deregulation of NF-kappaB in diffuse large B-cell lymphoma. *Nature* **459**, 717-721 (2009).

3. R. D. Morin, M. Mendez-Lago, A. J. Mungall, R. Goya, K. L. Mungall, R. D. Corbett, N. A. Johnson, T. M. Severson, R. Chiu, M. Field, S. Jackman, M. Krzywinski, D. W. Scott, D. L. Trinh, J. Tamura-Wells, S. Li, M. R. Firme, S. Rogic, M. Griffith, S. Chan, O. Yakovenko, I. M. Meyer, E. Y. Zhao, D. Smailus, M. Moksa, S. Chittaranjan, L. Rimsza, A. Brooks-Wilson, J. J. Spinelli, S. Ben-Neriah, B. Meissner, B. Woolcock, M. Boyle, H. McDonald, A. Tam, Y. Zhao, A. Delaney, T. Zeng, K. Tse, Y. Butterfield, I. Birol, R. Holt, J. Schein, D. E. Horsman, R.

Moore, S. J. Jones, J. M. Connors, M. Hirst, R. D. Gascoyne, M. A. Marra, Frequent mutation of histone-modifying genes in non-Hodgkin lymphoma. *Nature* **476**, 298-303 (2011).

4. J. Zhang, V. Grubor, C. L. Love, A. Banerjee, K. L. Richards, P. A. Mieczkowski, C. Dunphy, W. Choi, W. Y. Au, G. Srivastava, P. L. Lugar, D. A. Rizzieri, A. S. Lagoo, L. Bernal-Mizrachi, K. P. Mann, C. Flowers, K. Naresh, A. Evens, L. I. Gordon, M. Czader, J. I. Gill, E. D. Hsi, Q. Liu, A. Fan, K. Walsh, D. Jima, L. L. Smith, A. J. Johnson, J. C. Byrd, M. A. Luftig, T. Ni, J. Zhu, A. Chadburn, S. Levy, D. Dunson, S. S. Dave, Genetic heterogeneity of diffuse large B-cell lymphoma. *Proc Natl Acad Sci U S A* **110**, 1398-1403 (2013).

5. J. G. Tate, S. Bamford, H. C. Jubb, Z. Sondka, D. M. Beare, N. Bindal, H. Boutselakis, C. G. Cole, C. Creatore, E. Dawson, P. Fish, B. Harsha, C. Hathaway, S. C. Jupe, C. Y. Kok, K. Noble, L. Ponting, C. C. Ramshaw, C. E. Rye, H. E. Speedy, R. Stefancsik, S. L. Thompson, S. Wang, S. Ward, P. J. Campbell, S. A. Forbes, COSMIC: the Catalogue Of Somatic Mutations In Cancer. *Nucleic Acids Res*, (2018).

6. L. Pasqualucci, V. Trifonov, G. Fabbri, J. Ma, D. Rossi, A. Chiarenza, V. A. Wells, A. Grunn, M. Messina, O. Elliot, J. Chan, G. Bhagat, A. Chadburn, G. Gaidano, C. G. Mullighan, R. Rabadan, R. Dalla-Favera, Analysis of the coding genome of diffuse large B-cell lymphoma. *Nat Genet* **43**, 830-837 (2011).

7. J. de Jong, J. Sukbuntherng, D. Skee, J. Murphy, S. O'Brien, J. C. Byrd, D. James, P. Hellemans, D. J. Loury, J. Jiao, V. Chauhan, E. Mannaert, The effect of food on the pharmacokinetics of oral ibrutinib in healthy participants and patients with chronic lymphocytic leukemia. *Cancer Chemother Pharmacol* **75**, 907-916 (2015).

8. C. Yang, P. Lu, F. Y. Lee, A. Chadburn, J. C. Barrientos, J. P. Leonard, F. Ye, D. Zhang, D. M. Knowles, Y. L. Wang, Tyrosine kinase inhibition in diffuse large B-cell lymphoma:

molecular basis for antitumor activity and drug resistance of dasatinib. *Leukemia* **22**, 1755-1766 (2008).

9. G. Y. Di Veroli, C. Fornari, D. Wang, S. Mollard, J. L. Bramhall, F. M. Richards, D. I. Jodrell, Combenefit: an interactive platform for the analysis and visualization of drug combinations. *Bioinformatics* **32**, 2866-2868 (2016).

10. T. C. Chou, P. Talalay, Quantitative analysis of dose-effect relationships: the combined effects of multiple drugs or enzyme inhibitors. *Adv Enzyme Regul* **22**, 27-55 (1984).

11. H. Dai, S. Ehrentraut, S. Nagel, S. Eberth, C. Pommerenke, W. G. Dirks, R. Geffers, S. Kalavalapalli, M. Kaufmann, C. Meyer, S. Faehnrich, S. Chen, H. G. Drexler, R. A. MacLeod, Genomic Landscape of Primary Mediastinal B-Cell Lymphoma Cell Lines. *PLoS One* **10**, e0139663 (2015).

12. K. L. Meerbrey, G. Hu, J. D. Kessler, K. Roarty, M. Z. Li, J. E. Fang, J. I. Herschkowitz, A. E. Burrows, A. Ciccia, T. Sun, E. M. Schmitt, R. J. Bernardi, X. Fu, C. S. Bland, T. A. Cooper, R. Schiff, J. M. Rosen, T. F. Westbrook, S. J. Elledge, The pINDUCER lentiviral toolkit for inducible RNA interference in vitro and in vivo. *Proc Natl Acad Sci U S A* **108**, 3665-3670 (2011).

13. A. L. Szymczak, C. J. Workman, Y. Wang, K. M. Vignali, S. Dilioglou, E. F. Vanin, D. A. Vignali, Correction of multi-gene deficiency in vivo using a single 'self-cleaving' 2A peptide-based retroviral vector. *Nat Biotechnol* **22**, 589-594 (2004).

14. J. Schindelin, I. Arganda-Carreras, E. Frise, V. Kaynig, M. Longair, T. Pietzsch, S. Preibisch, C. Rueden, S. Saalfeld, B. Schmid, J. Y. Tinevez, D. J. White, V. Hartenstein, K. Eliceiri, P. Tomancak, A. Cardona, Fiji: an open-source platform for biological-image analysis. *Nat Methods* **9**, 676-682 (2012).

15. I. Appelmann, C. D. Rillahan, E. de Stanchina, G. Carbonetti, C. Chen, S. W. Lowe, C. J. Sherr, Janus kinase inhibition by ruxolitinib extends dasatinib- and dexamethasone-induced remissions in a mouse model of Ph+ ALL. *Blood* **125**, 1444-1451 (2015).